

# Steel Corrosion Inhibition by *Bupleurum lancifolium* (Apiaceae) Extract in Acid Solution

M. Benahmed · I. Selatnia · A. Achouri · H. Laouer ·  
N. Gherraf · S. Akkal

Received: 24 July 2013 / Accepted: 28 October 2014 / Published online: 19 November 2014  
© The Indian Institute of Metals - IIM 2014

**Abstract** The ethyl acetate extract of the aerial parts of *Bupleurum lancifolium* (Apiaceae) is tested as corrosion inhibitor of carbon steel (API 5L Gr B) in 1.0 M HCl and 0.5 M H<sub>2</sub>SO<sub>4</sub> solutions using weight loss measurement, electrochemical impedance spectroscopy and potentiodynamic polarization techniques. The results revealed that the corrosion inhibition efficiency increases with increasing extract concentration. Potentiodynamic polarization curves indicated that the plant extract behaves as a mixed-type inhibitor. The adsorption of inhibitor on carbon steel surface was found to follow Langmuir isotherm. The effect of temperature on the corrosion behavior of API 5L Gr B steel in acid solutions with and without plant extract was studied in the range 293–333 K. Surface analyses via scanning electron microscope shows a significant improvement on the surface morphology of the steel.

**Keywords** Corrosion inhibition · Carbon steel · Adsorption · *Bupleurum lancifolium*

## 1 Introduction

Many metals and alloys are used in different human activities. Carbon steel, the most widely used engineering material, accounts for approximately 85 % of the annual steel production worldwide. It is frequently used in wide industrial applications such as transport materials, marine applications, nuclear power and fossil fuel power plants, transportation, chemical processing, packaging, petroleum production and refining, pipelines, mining, construction, metal-processing equipment, household appliances, and so forth. The corrosion of steel and other metals is heightened in the presence of aggressive media such as acid. This process can lead to high economic losses. Therefore many industrial processes require the use of inhibitors to combat this natural phenomenon which may lead under special circumstances to severe industrial disasters such as in natural gas industry. Most of the well-known acid inhibitors used to restrain the metal corrosion are organic compounds especially those with electron donating groups: N, O and S which exhibited an effective corrosion inhibition by adsorption on the metal surface, thereby blocking the active sites and reducing the corrosion rate. Nevertheless, the use of synthetic inhibitors is more and more limited owing to their harmful effect on the environment [1–3].

In the recent years, there is an increasing awareness towards environment preservation by looking for eco-friendly and green chemicals to substitute the hazardous ones. In fact, many studies were carried out to investigate some naturally occurring substances, as corrosion inhibitors for different metals in various environments, instead of

---

M. Benahmed (✉) · I. Selatnia  
Laboratoire des molécules bioactives et applications, Université  
Tébessa, Route de Constantine, 12000 Tébessa, Algeria  
e-mail: riad43200@yahoo.fr

A. Achouri · S. Akkal  
Laboratoire de Phytochimie et Analyses physicochimiques et  
Biologiques, Département de Chimie, Faculté de Sciences  
exactes, Université Mentouri Constantine, Route d'Ain el Bey,  
25000 Constantine, Algeria

H. Laouer  
Laboratoire de Valorisation des Ressources Naturelles  
Biologiques, Département de Biologie, Université Ferhat Abbas  
de Sétif, Sétif, Algeria

N. Gherraf  
Laboratoire des Ressources Naturelles et Aménagement des  
milieux sensibles, Université Larbi ben M'hidi, Oum El  
Bouaghi, Algeria

the detrimental synthetic compounds [4–6]. In this context plant extracts may provide an incredibly rich source of natural chemical compounds which are nontoxic, biodegradable and readily available and can be extracted by simple procedures. For instance, the extracts of *Azadirachta indica* [7], *Olea europaea* [8], *Zanthoxylum alatum* [9] and *Ferula harmonis* [10] were studied as corrosion inhibitors in HCl and H<sub>2</sub>SO<sub>4</sub> medium.

The present work is devoted to test the ethylacetate extract of the aerial parts *Bupleurum lancifolium* (Apiaceae) as corrosion inhibitor for API 5L Gr B steel in 1.0 M HCl and 0.5 M H<sub>2</sub>SO<sub>4</sub> solutions. The genus *Bupleurum*, family Apiaceae, is widespread in the Mediterranean. The flora of Algeria involves 14 species of *Bupleurum* [11] amongst which *B. lancifolium* called “*Bou redim*” and widespread in all Algeria. Weight loss measurements, potentiodynamic polarization and electrochemical impedance spectroscopy methods were used to assess the inhibition efficiency of the extract. To the best of our knowledge no studies have been undertaken regarding the inhibitive effect of the plant in hand.

## 2 Experimental

### 2.1 Materials

Carbon steel (API 5L Gr B) samples having percent composition of 0.025 P, 0.015 S, 1.20 Mn, 0.24 C and remaining Fe were used in the present study. Samples of CS with dimensions (1.0 × 0.8 × 0.4 cm) and an exposed surface area of 3.04 cm<sup>2</sup> were used for weight loss measurements. For electrochemical measurements, a three electrode cell assembly consisting of a steel cube embedded in araldite with the bottom exposed surface area of 0.8 cm<sup>2</sup> as the working electrode, a platinum rode as counter electrode and a saturated calomel electrode (SCE) as a reference electrode. The samples were polished with emery paper of different grades: (600, 800, and 1,200) then degreased with acetone and rinsed with distilled water, before being immersed in the test solution.

### 2.2 Solutions

The corrosive solutions of 1.0 M HCl and 0.5 M H<sub>2</sub>SO<sub>4</sub> were prepared by dilution of AR grade 37 % HCl and 98 % H<sub>2</sub>SO<sub>4</sub> in distilled water. The used inhibitor concentration range was 100–700 ppm.

### 2.3 Preparation of *Bupleurum lancifolium* Extracts (BLE)

Aerial parts of *B. lancifolium* were extracted three times with boiling methyl alcohol (70 %). The methyl alcohol extract

was evaporated in vacuo. The concentrated solution was diluted with 250 ml of boiling water, before being filtered. The residue was successively treated with ethyl acetate and *n*-butanol. Then, the solvents were removed to afford *n*-butanol and ethyl acetate extracts [12–14]. This later was used directly to conduct the inhibition experiment.

### 2.4 Weight Loss Measurements

Experiments were realized under total immersion in stagnant aerated condition using 250 ml capacity beakers containing 150 ml of test solution at room temperature. The CS samples were weighed and suspended in the previous beaker. The weight loss of steel specimens was determined after 15 h of immersion. From the weight loss data, the inhibition efficiency IE (%) and surface coverage ( $\theta$ ) was calculated as follows [15].

$$IE\% = \frac{C_{r_0} - C_{r_i}}{C_{r_0}} \times 100 \quad (1)$$

$$\theta = \frac{C_{r_0} - C_{r_i}}{C_{r_0}} \quad (2)$$

where Cr<sub>0</sub> and Cr<sub>i</sub> are the corrosion rates in absence and presence of inhibitor, respectively.

### 2.5 Potentiodynamic Polarization Measurement

Polarization curve measurements were carried out using a PC controlled Volta Lab potentiostat (Model PGZ 301) system with Volta master 4 software, without and with addition of various solution concentrations of BLE (0, 100, 300, 500, and 700 ppm) at a scan rate of 1 mV/s. Open circuit potential E<sub>ocp</sub>, was measured for 30 min to allow stabilization of the steady state potential. The potential of potentiodynamic polarization curves was started from –250 to –1,000 mV. The inhibition efficiency IE (%) was calculated using the relation (3) [16]:

$$IE\% = \frac{I_{corr} - I_{corr(i)}}{I_{corr}} \times 100 \quad (3)$$

where I<sub>corr</sub> and I<sub>corr(i)</sub> are the corrosion current densities without and with the addition of the inhibitor respectively.

### 2.6 Electrochemical Impedance Spectroscopy (EIS)

The electrochemical impedance spectroscopy (EIS) measurements were carried out using the same instrument described above (Sect. 2.5) with the open circuit potential. E<sub>ocp</sub> of each sample was immersed for 30 min over a frequency range of 100 kHz–0.01 Hz with applied potential signal amplitude of 5 mV. The percentage inhibition efficiency IE (%) was calculated from:

$$IE\% = \frac{R_1 - R_2}{R_1} \times 100 \tag{4}$$

where  $R_1$  and  $R_2$  are charge transfer resistances of steel in uninhibited and inhibited solutions, respectively.

### 2.7 Scanning Electron Microscope (SEM)

Samples were prepared as described above. After immersion in acidic solutions without and with addition of 500 ppm of BLE at room temperature for 6 h, the samples were cleaned with distilled water, dried and then examined by TESCAN VEGA TS 5130 MM SEM.

## 3 Results and Discussion

### 3.1 Weight Loss Measurements

The weight loss method has found broad practical applications [17]. The rate of corrosion can be defined as the ratio of the loss in weight of the sample  $\Delta W$  to its area  $A$  and the time length over which the test was undertaken as given in Eq. (5) [18]. A major advantage of this method is its relative simplicity.

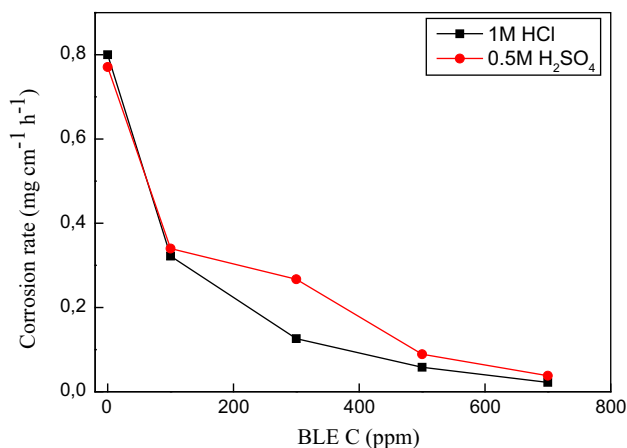


**Fig. 1** Relationship between corrosion rate and concentration of BLE in 1.0 M HCl and 0.5 M H<sub>2</sub>SO<sub>4</sub> at room temperature

$$Cr = \frac{\Delta W}{At} \tag{5}$$

The data obtained for the corrosion behavior of CS in 0.5 M H<sub>2</sub>SO<sub>4</sub> and 1 M HCl solutions containing different concentrations of the BLE from weight loss measurements are presented in Fig. 1 as well as Table 1. Figure 1 shows the corrosion rate as a function of the inhibitor concentration. It is observed that the corrosion rates decreased with the increase in concentration of BLE in both acidic media, indicating that the extent of inhibition is dependent upon the amount of extract present. The values of the percentage inhibition efficiency were determined for 15 h immersion period using Eq. 1. The results obtained are shown in Table 1 and indicate that the plant extract show a significant inhibitive effect on CS in 0.5 M H<sub>2</sub>SO<sub>4</sub> and 1 M HCl solutions. Addition of plant extract increases the inhibition efficiency in both acidic media. This indicates that the phytochemical components of the extract are adsorbed onto the steel surface resulting in the blocking of the reaction sites [17].

### 3.2 Adsorption Isotherm

In order to acquire more information about the mode of adsorption of the phytochemical components of the BLE on the surface of CS, the experimental data have been tested with several adsorption isotherms, including Langmuir, Frumkin and Temkin isotherms.

$$\text{Langmuir : } \frac{C}{\theta} = \frac{1}{k} + C \tag{6}$$

$$\text{Frumkin : } \log \left[ \frac{\theta}{(1 - \theta)C} \right] = \log k + g\theta \tag{7}$$

$$\text{Temkin : } \log \frac{\theta}{C} = \log k - g\theta \tag{8}$$

where  $\theta$  the surface coverage,  $k$  is the adsorption equilibrium constant,  $c$  is the concentration of inhibitor and  $g$  is the adsorbate parameter [19]. Again, the weight loss measurements were employed in this experiment with the concentration range 100, 300, 500, and 700 ppm at room temperature. The corresponding plots are shown in Fig. 2,

**Table 1** Effect of inhibitor concentration on inhibition efficiency of BLE in 1.0 M HCl and 0.5 M H<sub>2</sub>SO<sub>4</sub>

Conc. ppm	HCl			H <sub>2</sub> SO <sub>4</sub>		
	Corrosion rate (mg cm <sup>-2</sup> h <sup>-1</sup> )	$\theta$	IE (%)	Corrosion rate (mg cm <sup>-2</sup> h <sup>-1</sup> )	$\theta$	IE (%)
0	0.800	–	–	0.771	–	–
100	0.322	0.597	59.75	0.334	0.580	58.00
300	0.126	0.842	84.25	0.287	0.627	62.77
500	0.058	0.927	92.75	0.089	0.884	88.45
700	0.022	0.972	97.25	0.038	0.950	95.07

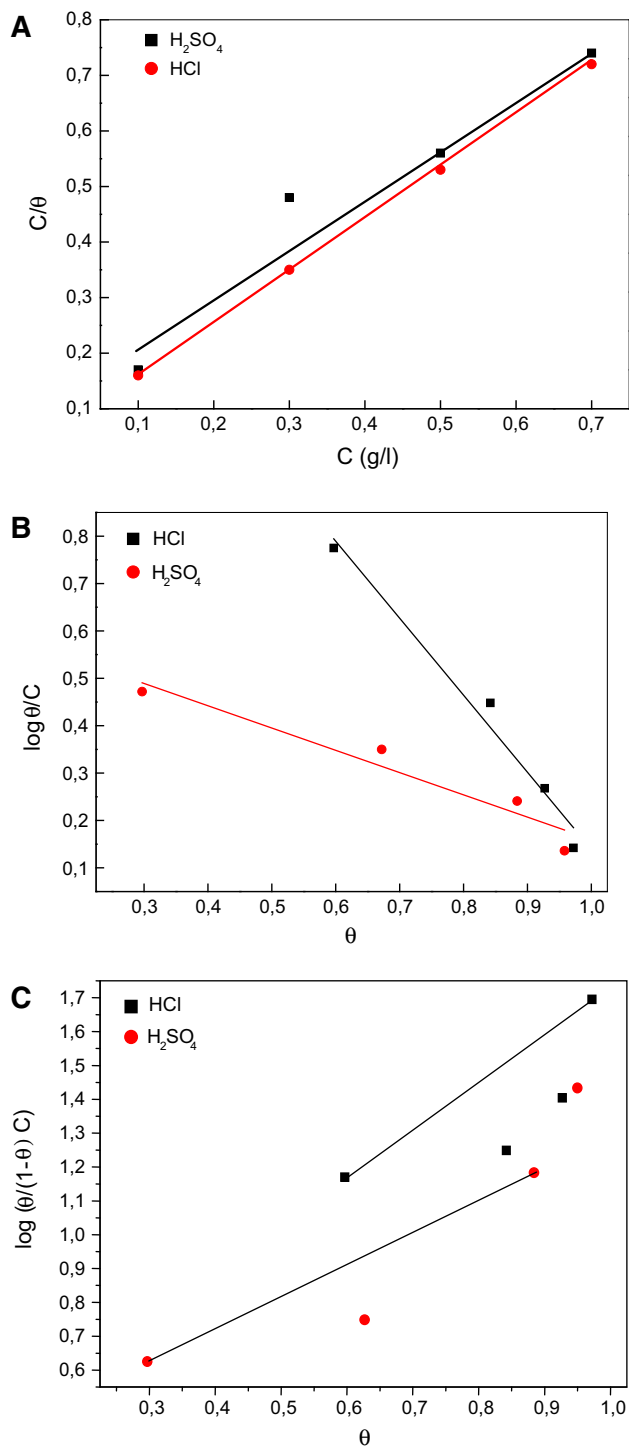


**Fig. 2** a Langmuir, b Temkin, and c Frumkin isotherm for the adsorption BLE on the surface of CS in 1 M HCl and 0.5 M H<sub>2</sub>SO<sub>4</sub>

where the  $r^2$  values for Langmuir isotherm (Fig. 2a) were 0.9999 in 1 M HCl and 0.9711 in 0.5 M H<sub>2</sub>SO<sub>4</sub>. For Temkin isotherm (Fig. 2b),  $r^2$  values were 0.9785 in 1 M HCl and 0.9411 in 0.5 M H<sub>2</sub>SO<sub>4</sub>. On the other hand, Frumkin isotherm (Fig. 2c) shows  $r^2$  values of 0.6596 in

**Table 2** Parameters of the straight lines of  $\frac{C}{\theta} - c$  (calculated from the data in Fig. 2a using Eq. (6))

Acid solution	Linear correlation coefficient (r)	Intercept (g/l)	K (l/g)
1 M HCl	0.9999	0.07	14.28
0.5 M H <sub>2</sub> SO <sub>4</sub>	0.9711	0.13	7.69

1 M HCl and 0.8648 in 0.5 M H<sub>2</sub>SO<sub>4</sub>. From this observation, it is concluded that Langmuir isotherm shows the best correlation with the experimental data in both 1.0 M HCl and 0.5 M H<sub>2</sub>SO<sub>4</sub> solutions. This isotherm assumes that the adsorbed molecules occupy only one site and there are no interactions with other adsorbed species [20]. Inspection of Table 2 shows that K value in 1.0 M HCl is higher than that in 0.5 M H<sub>2</sub>SO<sub>4</sub>, which indicates that BLE exhibits a stronger tendency to be adsorbed on steel surface in 1.0 M HCl solution [18]. It is worth to note that the discussion of the adsorption isotherm behavior using natural product extracts as inhibitors in terms of the standard free energy of adsorption value is not possible because the molecular mass of the extract component is not known. Some authors [21, 22], noted the same limitation in their studies on acid corrosion with some plant extracts.

### 3.3 Polarization Curves

From the anodic and cathodic polarization curves (Figs. 3 and 4) of CS in 1 M HCl and 0.5 M H<sub>2</sub>SO<sub>4</sub> media at different concentrations of BLE, various electrochemical parameters were computed and listed in Table 3. From the corrosion current density ( $i_{\text{corr}}$ ) values, the inhibition efficiency was calculated as in Eq. (3).

In 1.0 M HCl solution, the presence of BLE causes a remarkable decrease in the corrosion rate i.e., shifts both the anodic and cathodic curves to lower current densities (Fig. 3). In other words, both cathodic and anodic reactions of the steel electrode are retarded by the extract in hydrochloric acid solution. On the other hand, in 0.5 M H<sub>2</sub>SO<sub>4</sub> solution, *B. lancifolium* extract prominently inhibits the anodic reaction while has slight inhibitive effect on cathodic reaction (Fig. 4). Inspection of Table 3 reveals that in the presence of inhibitor, the values of corrosion current density ( $i_{\text{corr}}$ ) were decreased in both acids. Correspondingly, EI (%) increases with the inhibitor concentration. The inhibition efficiency of 700 ppm plant extract reaches up to a maximum of 97.48 % in 1.0 M HCl; and 82.79 % in H<sub>2</sub>SO<sub>4</sub>. This behavior reflects its ability to inhibit the corrosion of carbon steel in both acidic solutions. Moreover, it can be observed that the addition of the inhibitor causes no change in the anodic and cathodic Tafel slopes leading to the fact that inhibitor is first adsorbed

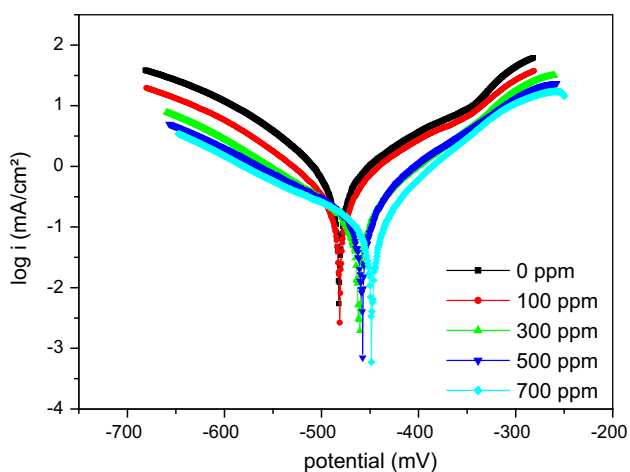


**Fig. 3** Potentiodynamic polarization curves for CS in 1 M HCl without and with different concentration of BLE

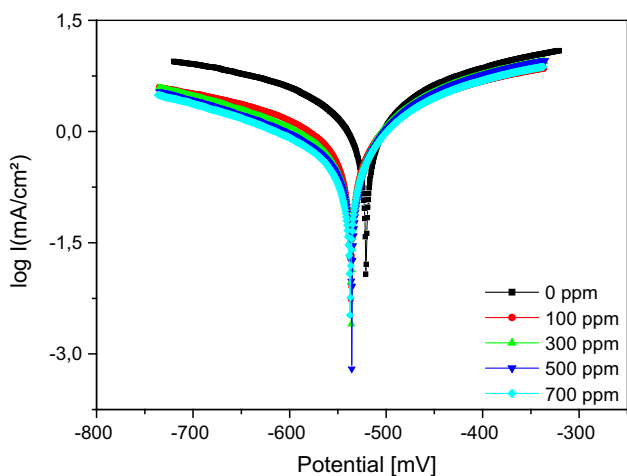


**Fig. 4** Potentiodynamic polarization curves for CS in 0.5 M H<sub>2</sub>SO<sub>4</sub> without and with different concentration of BLE

onto steel surface and therefore impedes by merely blocking the reaction sites of iron surface [23].

### 3.4 Electrochemical Impedance Spectroscopy

Figures 5 and 6 illustrate the Nyquist diagrams for the CS in 1.0 M HCl and 0.5 M H<sub>2</sub>SO<sub>4</sub> at 25 °C, respectively. In both acid solutions, the impedance diagrams display one single capacitive loop indicating that the corrosion of steel is mainly controlled by a charge transfer process [24]. All capacitive loops are not perfect semicircles which can be attributed to the frequency dispersion effect as a result of the roughness and inhomogeneous of electrode surface [25]. Furthermore, the size of these capacitive loops increases on increasing the plant extract concentration. This suggested that the formed inhibitive film was strengthened by addition of plant extract [9].

The EIS results of these plots are simulated by the equivalent circuit shown in Fig. 7, to a simple model including the solution resistance (R<sub>s</sub>) and the double layer capacitance (C<sub>dl</sub>) placed in parallel to charge transfer resistance R<sub>ct</sub>. The electrochemical parameters of C<sub>dl</sub> and R<sub>ct</sub> whose value is a measure of electron transfer across the surface is inversely proportional to corrosion rate [26] are listed in Table 4. Inspection of data in Table 4 shows clearly that R<sub>ct</sub> increases prominently while C<sub>dl</sub> decreases with the concentration of BLE in both acids. The greatest inhibitive effect is observed at 700 ppm of BLE showing an R<sub>ct</sub> value of 1,036 Ω cm<sup>2</sup> in 1.0 M HCl, and 134.6 Ω cm<sup>2</sup> in 0.5 M H<sub>2</sub>SO<sub>4</sub>; and a C<sub>dl</sub> value of 54.64 μF cm<sup>-2</sup> in 1.0 M HCl, and 74.71 μF cm<sup>-2</sup> in 0.5 M H<sub>2</sub>SO<sub>4</sub>. The decrease in capacity with increasing plant extract concentration may be attributed to the formation of a protective layer on the electrode surface [25].

**Table 3** The polarization parameter values of the corrosion of CS in 1 M HCl and 0.5 M H<sub>2</sub>SO<sub>4</sub> solution containing different concentrations of BLE

Acid solution	Conc. of BLE (ppm)	-E <sub>corr</sub> (mV)	I <sub>corr</sub> (mA cm <sup>-2</sup> )	β <sub>a</sub> (mV)	-β <sub>c</sub> (mV)	IE (%)
0.1 M HCl	0	481.6	2.9973	149.0	178.6	-
	100	481.3	1.1600	131.6	159.80	61.02
	300	475.0	0.3982	108.9	207.5	86.71
	500	458.5	0.2328	90.8	148.8	92.23
	700	450.1	0.0754	65.6	116.1	97.48
0.5 M H <sub>2</sub> SO <sub>4</sub>	0	520.3	2.5458	276.6	344.7	-
	100	536.3	1.1260	210.7	350.6	55.77
	300	536.1	0.5150	96.5	192.7	79.77
	500	535.2	0.5090	112	255	80.00
	700	537.4	0.4374	99.5	208.9	82.79

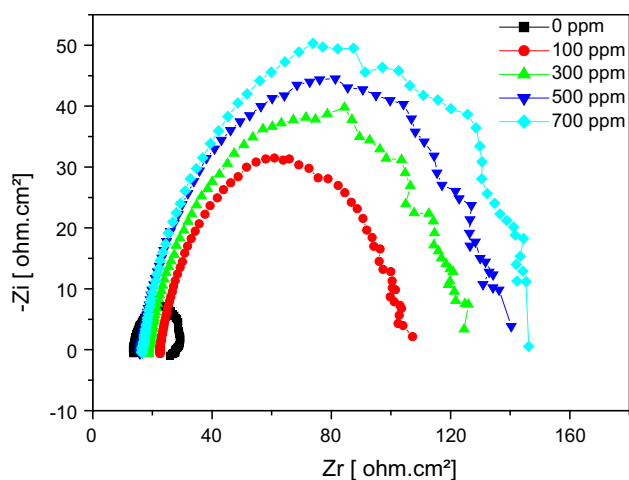


**Fig. 5** Nyquist plots for CS in 0.5 M H<sub>2</sub>SO<sub>4</sub> with different concentration of BLE

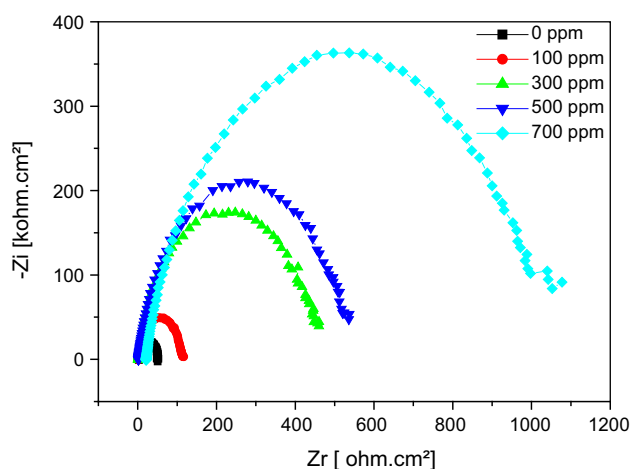


**Fig. 6** Nyquist plots for CS in 1.0 M HCl with different concentration of BLE

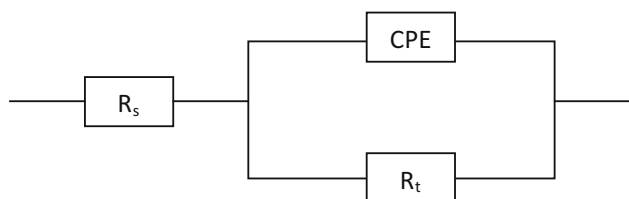


**Fig. 7** Equivalent circuit model

### 3.5 Effect of Temperature

The effect of temperature on the corrosion of CS in free and inhibited acidic solutions was studied using potentiostatic polarization in the range of 293–333 K (Fig. 8). The acid solutions were inhibited by addition of 500 ppm of BLE. The corrosion parameters calculated from the

**Table 4** Impedance parameters with corresponding inhibition efficiency for the corrosion of CS in 1.0 M HCl and 0.5 M H<sub>2</sub>SO<sub>4</sub> at different concentrations of BLE

Acid solution	Conc. (ppm)	C <sub>dl</sub> (μF cm <sup>-2</sup> )	R <sub>ct</sub> (Ω cm <sup>2</sup> )	IE (%)
1.0 M HCl	0	207.6	48.44	–
	100	158.7	112.2	56.82
	300	152.8	468.7	89.66
	500	131.8	540.7	91.04
	700	54.64	1,036	95.32
0.5 M H <sub>2</sub> SO <sub>4</sub>	0	186.8	13.46	–
	100	94.39	84.29	81.65
	300	72.47	109.7	87.73
	500	64.90	122.6	89.02
	700	74.71	134.6	90.00

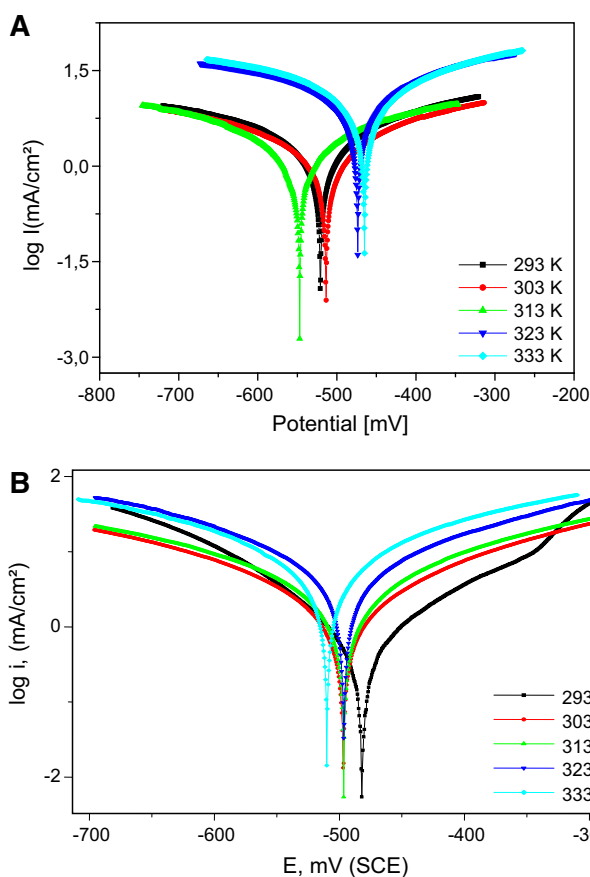


**Fig. 8** Effect of temperature on the cathodic and anodic responses CS in: **a** 0.5 M H<sub>2</sub>SO<sub>4</sub> and **b** 1 M HCl

polarization curves are given in Table 5. Inspection of Table 5 reveals that, in both acid solutions, the corrosion current density (*i<sub>corr</sub>*) in both free and inhibited acid media increased with increasing temperature. However, the inhibition efficiency BLE decreases markedly with increasing temperature.



**Table 5** Corrosion parameters of CS in solutions of acid solutions free and inhibited by 500 ppm of BLE at different temperatures

Temp. (K)	Solution	H <sub>2</sub> SO <sub>4</sub>			HCl		
		−E <sub>corr</sub> (mV)	I <sub>corr</sub> (mA cm <sup>−2</sup> )	IE (%)	−E <sub>corr</sub> (mV)	I <sub>corr</sub> (mA cm <sup>−2</sup> )	IE (%)
293	Free	520.3	2.5458	–	481.6	2.9973	–
	Inhibited	535.2	0.5090	80.00	458.5	0.2328	92.23
303	Free	513.7	3.0742	–	496.8	4.0305	–
	Inhibited	528.4	1.2214	60.26	461.6	0.3436	91.47
313	Free	468.5	5.0219	–	496.4	5.1180	–
	Inhibited	516.2	2.8338	49.57	494.9	1.7624	69.25
323	Free	473.7	13.9195	–	496.3	5.7321	–
	Inhibited	484.3	7.0072	43.65	489.6	1.6552	67.65
333	Free	465.1	15.0804	–	509.9	12.6402	–
	Inhibited	484.3	9.8831	34.46	502.8	4.0235	68.16

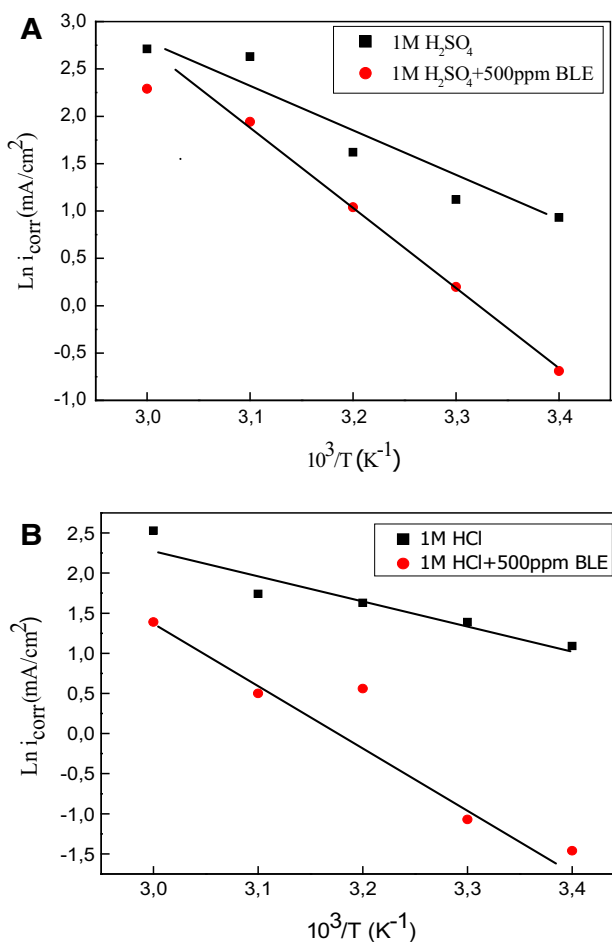


**Fig. 9** Arrhenius plots of corrosion  $\ln i_{corr}$  Vs  $1/T$  of: **a** 0.5 M H<sub>2</sub>SO<sub>4</sub> and 0.5 M H<sub>2</sub>SO<sub>4</sub> + 500 ppm BLE. **b** 1 M HCl and 1 M HCl + 500 ppm BLE

The activation energies of the corrosion process in free and inhibited solutions were calculated using the Arrhenius equation

**Table 6** Activation parameters of CS in acid solutions with and without BLE

Acid solution	E <sub>a</sub> (KJ/mol)
1 M HCl	25.71
1 M HCl + 500 ppm BLE	59.37
0.5 M H <sub>2</sub> SO <sub>4</sub>	40.80
0.5 M H <sub>2</sub> SO <sub>4</sub> + 500 ppm BLE	62.32

$$I_{corr} = k \exp\left(-\frac{E_a}{RT}\right) \tag{9}$$

where E<sub>a</sub> is the activation energy, T is the absolute temperature, k is the Arrhenius pre-exponential constant and R is the universal gas constant. This equation can be used to calculate the E<sub>a</sub> values of the corrosion reaction without and with BLE. Plotting the natural logarithm of the corrosion current density versus 1/T gives a straight line, as revealed by Fig. 9. The calculated values of the activation energy in the absence and presence of BLE in both acid solutions are listed in Table 6. Inspection of Table 6 reveals that the values of E<sub>a</sub> in presence of 500 ppm BLE were higher than those in absence of the inhibitor in both acid solutions. The increase in the E<sub>a</sub> may be interpreted as physical adsorption that occurs in the first stage [27]. The activation energy values of the inhibitor are 59.37 and 62.32 kJ/mol in 1 M HCl and 0.5 M H<sub>2</sub>SO<sub>4</sub> solutions respectively, which confirmed the assertion that the inhibition of steel is by physical adsorption [28]. Furthermore, the increase of the activation energy can be attributed to an appreciable decrease in the adsorption of the inhibitor on the steel surface with increasing temperature [21]. As adsorption decreases more desorption of inhibitor molecules occurs because these two opposite processes are in equilibrium. Due to more desorption of inhibitor molecules, an important surface, the steel comes in contact with aggressive solution.

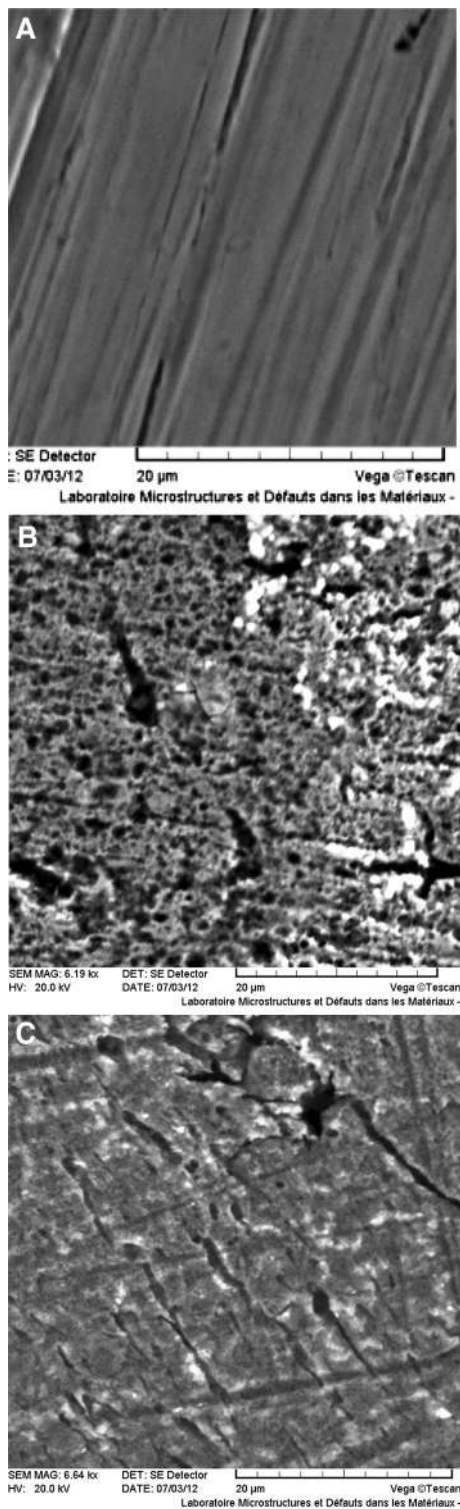


**Fig. 10** SEM micrographs of: **a** Untreated steel, **b** CS treated with 1 M HCl, **c** CS treated with 1 M HCl + 500 ppm of BLE

### 3.6 Scanning Electron Microscopy (SEM)

Surface examination using SEM (Fig. 10) was carried out to investigate the effect of inhibitor on the surface

morphology of the steel. Figure 10b reveals that the steel surface after immersion in uninhibited 1 M HCl solution for 6 h displays an aggressive attack of the corroding medium. On the other hand, a smooth surface was observed in the inhibited solution (Fig. 10c).

## 4 Conclusions

- The ethyl acetate extract of *B. lancifolium* inhibits the CS corrosion in HCl and H<sub>2</sub>SO<sub>4</sub> solutions.
- The inhibition efficiency increases with increasing extract concentration and decreases with increasing temperature.
- The adsorption of extract components follows Langmuir adsorption isotherm.
- Nyquist plots of CS in HCl and H<sub>2</sub>SO<sub>4</sub> solutions containing plant extracts shows that charge transfer resistance increases with increasing of plant extract concentration.

## References

1. Bentiss F, Traisnel M, and Lagrenee M, *Corros Sci* **42** (2000) 127.
2. Allaoui M, Cheriti A, Gherraf N, Chebouat E, Dadamoussa B, and Salhi R, *Int J Electrochem Sci* **8** (2013) 9429.
3. El ayyachy M, El Idrissi A, and Hammouti B, *Corros Sci* **48** (2006) 2470.
4. El-Etre A Y, *Corros Sci* **43** (2001) 1031.
5. El-Etre A Y, *Corros Sci* **40** (1998) 1845.
6. Bouyanzer A, Hammouti B, and Majidi L, *Mater Lett* **60** (2006) 2840.
7. Valek A, and Martinez S, *Corros Sci* **61** (2007) 148.
8. El-Etre A Y, *Corros Sci*, **314** (2007) 578.
9. Chauhan L R, and Gunasekaran G, *Corros Sci* **49** (2007) 1143.
10. El-Etre A Y, *Corros Sci* **108** (2008) 278.
11. Quezel P, and Santa S, *Nouvelle flore de l'Algérie et des régions désertiques méridionales*, Tome II, Editions du Centre National de la Recherche Scientifique, Paris (1963).
12. Benahmed M, Akkal S, Louaar S, Laouer H, and Duddeck H, *Biochem Syst Ecol* **34** (2006) 645.
13. Benahmed M, Akkal S, Elomri A, Laouer H, Vérité P, and Seguin E *Arab J Chem* (in press).
14. Akkal S, Louaar S, Benahmed M, Laouer H, and Duddeck H, *Chem Nat Comp* **46** (2010) 719.
15. Orubite K O, and Oforka N C, *Mater Lett* **58** (2004) 1768.
16. El-Etre A Y, *App Surf Sci* **252** (2006) 8521.
17. Umoren S A, and Eduok U M, Solomon M M, and Udoh A P, *Arab J Chem* (in press).
18. Deng S, and Li X, *Corros Sci* **55** (2012) 407.
19. Hussin Hazwan M, and kassim M, *Mater Chem phys* **125** (2011) 461.
20. Ali Sk A, Saeed M T, and Rahman S U, *Corros Sci* **45** (2003) 253.
21. Lebrini M, Robert F, Lecante A, and Roos C, *Corros Sci* **53** (2011) 687.



22. Satapathy A K, Gunasekaran G, Sahoo S C, Kumar A, and Rodrigues P V, *Corros Sci* **51** (2009) 2848.
23. Behpour M, Ghoreishi S M, Khayatkashani M, and Soltani N, *Mater Chem Phys* **131** (2012) 621.
24. Behpour M, Ghoreishi S M, Mohamadi N, and Soltani N, *Corros Sci* **52** (2010) 4046.
25. Lebrini M, Lagrenee M, Vezin H, Traisnel M, and Bentiss F, *Corros Sci* **49** (2007) 2254.
26. Abdel-Gaber A M, Abd-El-Nabey B A, Sidahmed I M, and El-Zayady A M, *Corros Sci* **48** (2006) 2765.
27. Martinez S, and Stern I, *Appl Surf Sci* **199** (2002) 83.
28. Uwah I E, Okafor P C, and Ebiekpe V E, *Arab J Chem* (in press).